

Seismic Performance Assessment of a Tied Arch Concrete Filled Steel Tubular (CFST) bridge

Niyog Uprety ^a, Rajan Suwal ^b

^a Department of Civil Engineering, Thapathali Campus, IOE, Tribhuvan University, Nepal

^b Department of Civil Engineering, Pulchowk Campus, IOE, Tribhuvan University, Nepal

✉ ^a upretyniyog13@gmail.com, ^b rajan.suwal@ioe.edu.np

Abstract

CFST bridges are widely used in long-span bridges due to their high strength, stiffness, and durability. In the context of Nepal, CFST bridges can play a significant role in meeting the country's growing demand for modern infrastructure. The main objective of this study is to evaluate the seismic performance of an hypothetical Tied Arch Concrete Filled Tubular (CFST) bridge under various ground motions. Seven different earthquake time histories are taken as the seismic input for this study. The pushover analysis was utilized to ascertain the bridge's displacement capacity. Non-Linear Time History Analysis (NTHA) are performed on the transverse direction of the bridge to determine the displacement demand of the bridge. It is found that the seismic capacity of the bridge far exceeds the seismic demand.

Keywords

CFST, Finite Element, ANSYS

1. Introduction

1.1 Concrete Filled Steel Tube (CFST)

Concrete-filled steel tubular (CFST) structures are composite structures that consist of a steel tube filled with concrete [1]. These structures offer several advantages over conventional steel or concrete structures, including high strength, stiffness, durability, and excellent resistance to fire and corrosion. A typical circular CFST section is shown in figure 1.

CFST structures can be designed to resist both compressive and tensile loads, making them highly suitable for applications requiring high strength and stiffness. The combination of steel and concrete in CFST structures results in a structure that can withstand significant axial, bending, and shear stresses, making them ideal for use in seismic regions. When subjected to compressive loads, the steel tube confines the concrete, preventing it from crushing. This confinement increases the concrete's compressive strength and prevents premature failure, resulting in a more durable and resilient structure. The confinement effect also prevents the concrete from expanding laterally, resulting in reduced lateral deflection and improved stiffness. The concrete provides lateral support to the steel tube and prevents it from

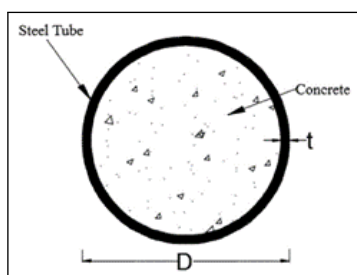


Figure 1: Typical Circular CFST section

buckling. The tube also serves as the formwork for the concrete during the construction stage [1, 2].

1.2 Concrete Filled Steel Tube (CFST) Arch Bridges

CFST arch bridges, constructed using concrete-filled steel tubes, have seen significant development since the first one was built in the Soviet Union in the 1930s, with the Wangcang Bridge in China in 1990 marking a turning point in their proliferation. As of October 2021, China had constructed or was in the process of building 484 CFST arch bridges, making them a preferred choice over traditional reinforced concrete and steel arch bridges. These bridges come in various types, including Deck Arch, Half-through Arch, Through deck-stiffened Arch, Through rigid-frame tied arch, and fly-bird-type arch [3]. They are shown in figure 2. CFST technology holds great promise for seismic-prone areas like Nepal, but proper seismic assessment remains imperative. Research has explored the design, construction, and performance of CFST arch bridges in China, with innovative modeling and analysis techniques, such as finite element analysis and modal flexibility, providing insights into optimizing these structures for seismic loads [4] [5]. This comprehensive review showcases the progress and challenges

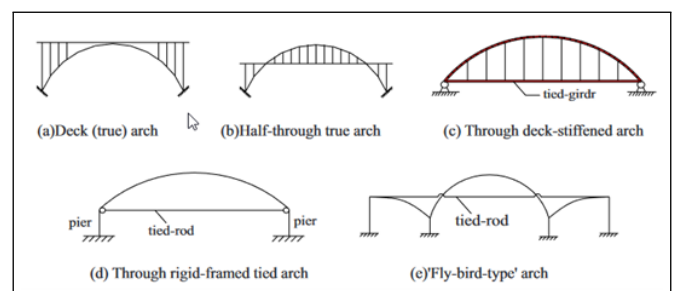


Figure 2: Types of CFST arch bridges

in the field of CFST arch bridges, offering valuable guidance for future design and construction endeavors.

The objective of this study was to perform performance assessment of Tied Girder CFST arch bridge. CFST (Concrete Filled Steel Tube) technology has the potential to be a great initiative for Nepal, which is located in a seismically active zone. CFST arch bridges have been proven to be ideal for long span bridges, which is especially important in as Nepal has deep gorges on which construction of piers is especially difficult. CFST arch bridges can be a great initiative for Nepal but as it lies in seismically active region, proper seismic assessment of such bridges would be a necessity.

2. Finite Element Modelling

2.1 Preliminary Design of the Tied Arch CFST Bridge

For the performance assessment of a hypothetical tied arch CFST bridge with a 70m span, typical member sizes were chosen based on common practice. The arch rib had a circular CFST with a diameter of 1.7m and a skin thickness of 25mm, while the bracing used a circular CFST with a diameter of 0.9m and a 16mm skin thickness. The tied girder was a prestressed box girder measuring 2.0m x 2.75m, and the end girder was a prestressed box girder sized at 2.9m x 3.25m. The hanger was made of 91-7mm high tensile strength wires, and the cross girder was comprised of prestressed T-girders with a depth of 2.4m. The bridge's deck slab and cantilever pedestrian slab, each with a thickness of 250mm, were assumed to be constructed from reinforced concrete. The section of Arch Rib, Bracing, End Girder and Tied Girder are shown in figure 3.

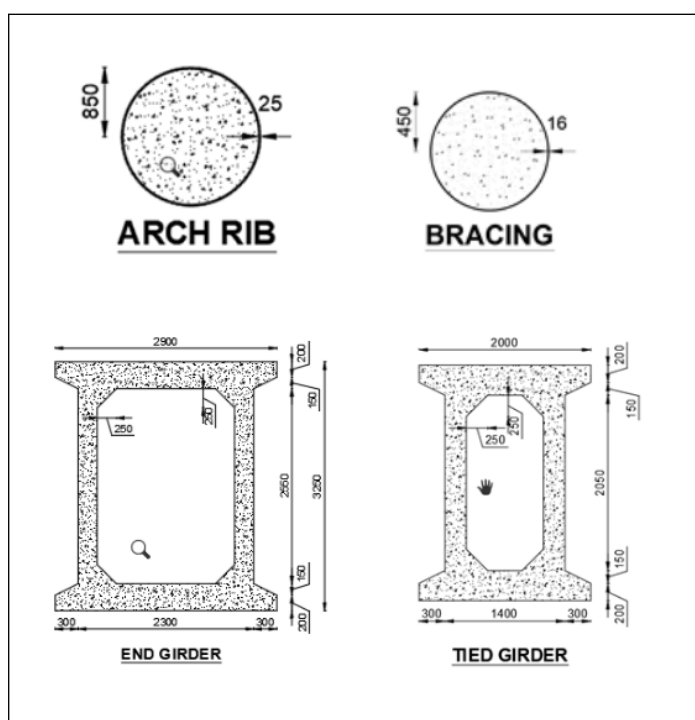


Figure 3: Typical Member Cross Sections of the Bridge

2.2 Bridge Modelling

The modeling of the arch bridge in ANSYS [6] followed a systematic approach. First, the 3D geometry of the bridge was created using the SpaceClaim Module within ANSYS Workbench. This step involved defining the structural shape and dimensions of the bridge. Once the geometry was established, the next crucial step was mesh generation. The mesh density and element types used were tailored to the complexity of the bridge's geometry and the required analysis accuracy. In this study, the mesh was automatically generated by ANSYS Mechanical.

For modeling different components of the bridge, specific element types were employed. The arch members and bracing were represented using 3D beam elements (BEAM188), which accounted for properties like cross-section, material characteristics, and orientation. Similarly, the main girders and cross girders were also modeled using 3D beam elements (BEAM188). To simulate the connections between the arch and the girders, joint elements like JOINT180 were utilized, capturing both rotational and translational constraints at these critical junctions. Additionally, the hanger for the bridge was modeled using tension-only elements (LINK180), designed to resist tension forces. Notably, to manage load transfer from the slab to the main girders, the slab itself was not explicitly modeled, and instead, the load from the slab was directly applied to the Cross Girder as a UDL (Uniformly Distributed Load). The bridge as modelled in ANSYS is shown in figure 4.

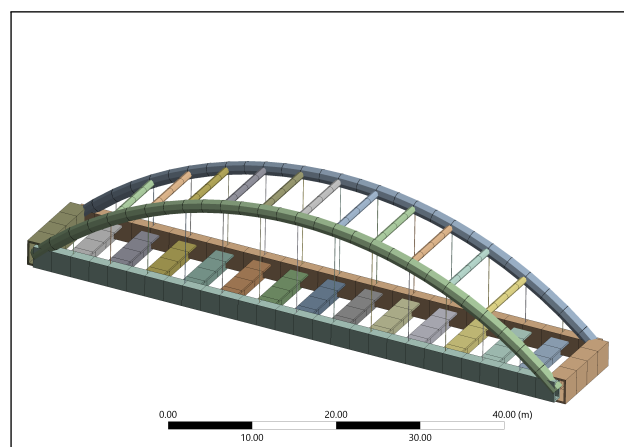


Figure 4: ANSYS Model of the Bridge

Equivalent section of CFST [7, 8, 5, 9] In the analysis of Concrete Filled Steel Tube (CFST) sections, the equivalent stiffness properties of the equivalent Concrete Section can be determined using the following formulas:

Equivalent Axial Stiffness (EA):

$$EA = E_c \cdot A_c + E_s \cdot A_s \tag{1}$$

where: EA is the equivalent axial stiffness of the CFST composite section, E_c is the Young's modulus of the concrete material, A_c is the cross-sectional area of the concrete, E_s is the Young's modulus of the steel material, and A_s is the cross-sectional area of the steel.

Equivalent Flexural Stiffness (EI):

$$EI = E_c \cdot I_c + E_s \cdot I_s \quad (2)$$

where: EI is the equivalent flexural stiffness of the CFST composite section, E_c is the Young's modulus of the concrete material, I_c is the moment of inertia of the concrete, E_s is the Young's modulus of the steel material, and I_s is the moment of inertia of the steel.

For the analysis, M40 concrete material properties based on the IS456 [10] standard were utilized. The failure mechanism for the concrete was modeled using the Menetrey-William Model [11]. The Menetrey-William model is a constitutive model for concrete that is based on the theory of plasticity with a non-associated flow rule. It accounts for Nonlinear stress-strain behavior, Dilatancy and Tensile Softening of the concrete. The properties used for CFST member using Menetrey-William Model is shown in Table 1. For the high-strength tensile wire, a steel material with a yield strength of 1500 MPa was employed. The plasticity criteria for the high tensile strength wire was characterized by bilinear isotropic hardening.

Table 1: Properties of Equivalent Material for CFST

Property	Value	Unit
Density	2462	kg/m ³
Young's Modulus	39.52	GPa
Poisson's Ratio	0.15	
Bulk Modulus	18.2	GPa
Shear Modulus	17.18	GPa
Menetrey-William Base		
Uniaxial Compressive Strength	40	MPa
Uniaxial Tensile Strength	4.42	MPa
Biaxial Compressive Strength	46.4	MPa
Dilatancy Angle	30	degrees
Softening		
Plastic Strain at Uniaxial Compressive Strength	0.001	
Ultimate Effective Plastic Strain in Compression	0.01	
Relative Stress at Start of Nonlinear Hardening	0.4	
Residual Compressive Relative Stress	0.2	
Plastic Strain Limit in Tension	0.001	
Residual Tensile Relative Stress	0.2	

The generation of mesh for the FEM model was done using the automatic mesh generation module provided in ANSYS. The solution technique for the Non-Linear Analysis was Newmark's method. The method of solution for the Newmark's method was Mode Superposition Method (MSUP). Maximum number of iteration for each time step was set as 10. The force convergence criteria for the model was set as Program Controlled.

3. Analysis And Results

Initially, a modal analysis was performed, followed by a pushover analysis in the transverse direction to determine the

bridge's displacement capacity. Subsequently, non-linear time history analysis was conducted to compute the displacement demand on the bridge in the transverse direction.

3.1 Modal Analysis

Modal analysis of the bridge is a dynamic analysis method utilized to determine its natural frequencies and corresponding mode shapes. In this study, a consideration of 20 modes enabled the identification of distinct vibrational patterns exhibited by the bridge under dynamic loading conditions. A 100% mass participation was achieved in the transverse direction through the incorporation of these 20 modes. The first ten frequency and period values for the bridge's modes are provided in the table 2.

Table 2: Bridge Modal Frequencies and Periods

Mode	Frequency (Hz)	Period (sec)
1	1.3433	0.7444
2	1.9623	0.5096
3	2.6412	0.3786
4	3.1354	0.3189
5	3.7019	0.2701
6	4.9902	0.2004
7	5.4078	0.1849
8	5.6534	0.1769
9	5.9796	0.1672
10	6.0107	0.1664

3.2 Pushover Analysis

Force-based pushover analysis was conducted in ANSYS to assess the bridge's response to lateral forces in the transverse direction. The analysis was executed in a step-by-step manner until convergence was achieved. Initially, incremental lateral forces were applied to the bridge model, and at each step, the corresponding displacements and base reaction were computed. The force was gradually increased until the convergence of the model was observed. The maximum displacement observed at this point was taken as the seismic demand for the bridge. Through the pushover analysis, the displacement capacity of the bridge was determined to be 235.21 mm, showcasing the maximum lateral displacement the structure could endure under progressively increasing forces.

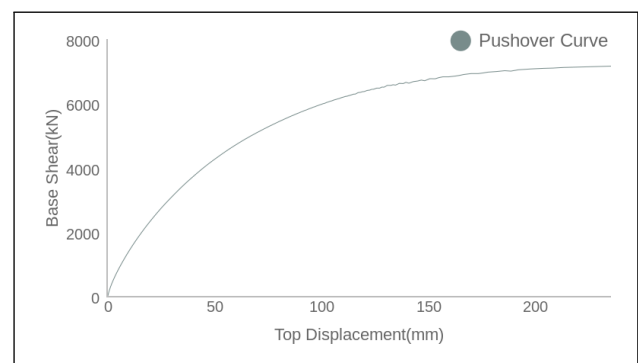


Figure 5: Pushover Curve

Figure 5 illustrates the pushover curve of the bridge,

graphically depicting the relationship between Base reaction and the corresponding displacements, providing valuable insights into the bridge’s structural capacity during lateral loading.

3.3 Non-Linear Time History Analysis

Nonlinear time history analysis was conducted for the bridge to assess its dynamic response under seismic conditions. Due to the unavailability of site-specific seismic data, six significant historical earthquakes were selected. These earthquake events were then matched to the IS 1893 [12] spectra to generate site-specific time histories for analysis. The earthquake time history used in this study is given in table 3. The unmatched and matched response spectra of the earthquakes are shown in figure 6 and figure 7 respectively.

Table 3: Historical Earthquake Data for Nonlinear Time History Analysis

SN	Name of Earthquake	Max Acceleration
1	Gorkha Earthquake	0.47152 g
2	Imperial Valley Earthquake	0.58624 g
3	Loma-Prieta Earthquake	0.52235 g
4	Northridge Earthquake	0.47644 g
5	Kobe Earthquake	0.53968 g
6	Kocaeli Earthquake	0.53873 g

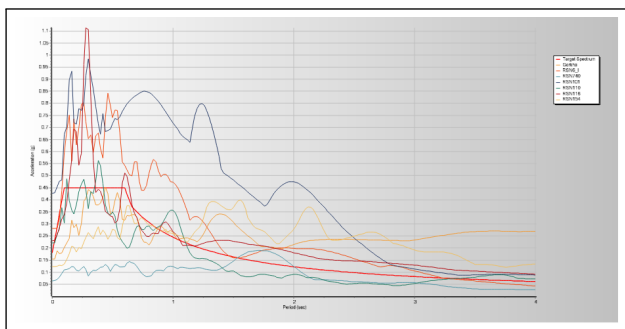


Figure 6: Unmatched Response Spectra

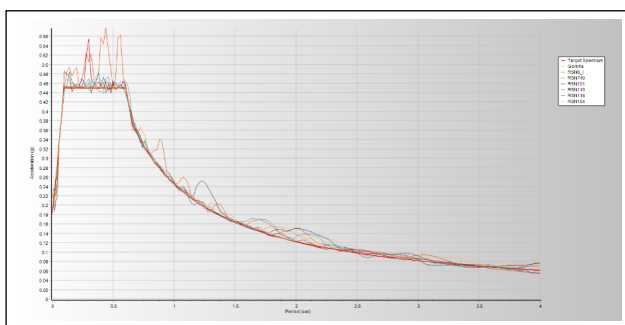


Figure 7: Matched Response Spectra

The displacement response of all the time history were calculated and were compared with the displacement demand obtained the time history analysis. The maximum displacement of all the time history is shown in table below. The displacment response of only gorkha earthquake is showm below to save space.

The displacement responses of all the time history records were calculated and subsequently compared with the displacement demand obtained from the Pushover analysis. The maximum displacements from each time history analysis are presented in the table 3.

Table 4: Maximum Displacement Responses from Time History Analysis

Earthquake	Max Displacement (mm)
Gorkha Earthquake	63.01
Imperial Valley Earthquake	83.04
Loma-Prieta Earthquake	62.68
Northridge Earthquake	64.94
Kobe Earthquake	70.48
Kocaeli Earthquake	65.46

Due to space constraints, the displacement response of only the Gorkha Earthquake is presented in figure 8 as an illustrative example.

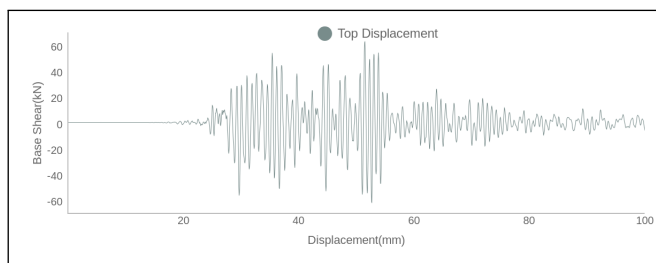


Figure 8: Displacement Response of Bridge to Gorkha Earthquake

The results from both time history and pushover analysis reveals critical insights into the structural behavior of the CFST arch bridge under seismic loading. The pushover analysis unveiled the bridge’s lateral displacement capacity, shedding light on its overall strength and ability to withstand lateral forces. This analysis, coupled with time history simulations using historical earthquake data, allowed for a comprehensive evaluation of the bridge’s response to dynamic excitations. The comparison of maximum displacements from time history analysis to displacement demands provided a crucial benchmark for assessing the structure’s seismic performance. Notably, the findings suggest that the CFST arch bridge exhibits robustness and promising resilience against a spectrum of historical earthquakes, showcasing its potential as a viable structural solution in seismic regions. This discussion underscores the significance of advanced analysis techniques in structural engineering and emphasizes the bridge’s suitability for areas prone to seismic activity.

4. Conclusions

- Modal analysis revealed the natural frequencies and mode shapes of the CFST arch bridge, providing insights into its vibrational characteristics.
- Force-based pushover analysis determined the bridge’s lateral displacement capacity, essential for understanding its response to lateral forces.

- Non-linear time history analysis, using a curated selection of historical earthquakes matched to IS1893 spectra, illuminated the bridge's dynamic response under seismic conditions.
- Maximum displacements from the analyses were compared to displacement demand, indicating the structure's seismic performance.
- The research findings suggest that the CFST arch bridge exhibits promising resilience against various historical earthquakes.
- This study highlights the significance of advanced modeling and analysis techniques for assessing CFST arch bridges, particularly in seismic regions, providing valuable insights for future bridge design and construction practices.

References

- [1] Baochun Chen, Junping Liu, and Jiangang Wei. *Concrete-Filled Steel Tubular Arch Bridges*. Springer, 2022. PDF.
- [2] R. Yadav. Parametric study on the axial behaviour of concrete filled steel tube (cfst) columns. *Am. J. Appl. Sci. Res.*, 3:21, 2017.
- [3] B. Chen and T.-L. Wang. Overview of concrete filled steel tube arch bridges in china. *Pract. Period. Struct. Des. Constr.*, 14(2):70–80, 2009.
- [4] Z. Xuhui, Q. Zhang, H. Sun, W. Ke, L. Ma, and L. Men. Seismic performance analysis of a concrete filled steel tubes arch bridge: A parametric study. *Eng. Rep.*, 2022.
- [5] C. Daihai, W. Wenze, Z. Li, Z. Xu, and F. Ma. Comparative analysis of seismic performance of 122-meter long concrete-filled steel tube arched chord truss bridge before and after reinforcement. *J. Asian Archit. Build. Eng.*, 19(2):90–102, 2020.
- [6] Inc. ANSYS. Ansys, 2023.
- [7] B. Jaishi, H.-J. Kim, M. K. Kim, W.-X. Ren, and S.-H. Lee. Finite element model updating of concrete-filled steel tubular arch bridge under operational condition using modal flexibility. *Mech. Syst. Signal Process.*, 21:2406–2426, 2007.
- [8] K. Bi, H. Hao, and W.-X. Ren. Seismic response of a concrete filled steel tubular arch bridge to spatially varying ground motions including local site effect. *Adv. Struct. Eng.*, 16(10):1799–1817, 2013.
- [9] J. Ma and Y. Li. Dynamic response analysis of half-through cfst arch bridges affected by crossbeams setting. *Adv. Eng. Forum*, 5:201–206, 2012.
- [10] Bureau of Indian Standards. *IS 456:2000: Plain and reinforced concrete - Code of practice*. Bureau of Indian Standards, 2000.
- [11] P. Menetrey and K.J. Willam. Triaxial failure criterion for concrete and its generalization. *ACI Struct. J.*, 92(3):311–318, 1995.
- [12] Indian Standards. *Is 1893:2016: Criteria for earthquake resistant design of structures*, 2016.